JOC*Article*

Aromatic C−H···O Interactions in a Series of Bindone Analogues. NMR and Quantum Mechanical Study

Mark Sigalov,*,† Alexander Vashchenko,‡ and Vladimir Khodorkovsky†,§

Department of Chemistry, Ben-Gurion University of the Negev, Beer-Sheva, 85104 Israel, Institute of Chemistry, Siberian Division of RAS, 664033 Irkutsk, Russia, and Université de la Méditerranée, UMR CNRS 6114, 13288, Marseille 09, France

msigalov@bgumail.bgu.ac.il

Received August 12, 2004

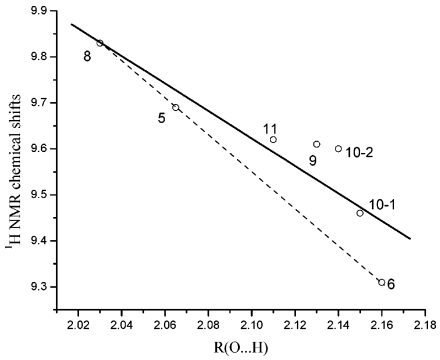

The aromatic C−H···O hydrogen bonding within the series of the structurally relative indenone derivatives has been studied. The presence of the hydrogen bonds is corroborated by the large low-field chemical shifts of the protons involved in the hydrogen bond observed experimentally and reproduced by quantum mechanical calculations. Further confirmation is provided by analysis of the orbital overlap coefficients, ^{13}C NMR chemical shifts, and one-bond spin−spin coupling constants $J(^{13}C-^{1}H)$. The relationship between molecular geometry and ^{1}H NMR chemical shifts of involved protons has a complex nature, but the C−H···O distance is the principal factor.

Introduction

The ability of the C−H group to act as a proton donor toward acceptors is currently recognized as one of the significant factors determining crystal structure patterns and molecular recognition phenomenon.[1−6]

Both inter- and intramolecular hydrogen bonds involving C−H···X interactions are well-known.[7−14] Various methods were applied to establish the presence of hydrogen bonding, among which analysis of short intermolecular contacts in solid state,[15−17] IR in solution[18,19] and in matrix,[20] NMR spectroscopy in solution,[7,21−24] and quantum mechanical calculations[14,21,22,25−27] should be mentioned.

† Ben-Gurion University of the Negev.
‡ Siberian Division of RAS.
§ Université de la Méditerranée.

(1) Taylor, R.; Kennard, O. *J. Am. Chem. Soc*. **1982**, *104*, 5063−5070.
(2) Desiraju, G. R., Ed. *The Crystal as Supramolecular Entity*; John Wiley & Sons: New York, 1996.
(3) Desiraju, G. R. *Acc. Chem. Res*. **1991**, *24*, 290−296.
(4) Desiraju, G. R. *Acc. Chem. Res*. **1996**, *29*, 441−449.
(5) Desiraju, G. R. *Science* **1997**, *278*, 404−405.
(6) Navon, O.; Bernstein, J.; Khodorkovsky, V. *Angew. Chem., Int. Ed. Engl.* **1997**, *36*, 601−603.
(7) Bruce, R. St. L.; Cooper, M. K.; Freeman, H. C.; McGrath, B. G. *Inorg. Chem*. **1974**, *13*, 1032−1037. Sammes, M. P.; Harlow, R. L.; Simonsen, S. H. *J. Chem. Soc., Perkin Trans. 2* **1976**, 1126−1135; Li, C.; Sammes, M. P. *J. Chem. Soc. Perkin Trans. 1* **1983**, 2193-2196.
(8) Novoa, J. J.; Mota, F. *Chem. Phys. Lett*. **1997**, *266*, 23−30.
(9) Reiling, S.; Brickmann, J.; Schlenkrich, M.; Bopp, P. A. *J. Comput. Chem*. **1996,** *17*, 133−147.
(10) Law, R. V.; Sasanuma, Y. *J. Chem. Soc., Faraday Trans*. **1996**, *92*, 4885−4888.
(11) Bertolasi, V.; Gilli, P.; Ferretti, V.; Gilli, G. *J. Chem. Soc., Perkin Trans. 2* **1997**, 945−952.
(12) Novoa, J. J.; Lafuente P.; Mota, F. *Chem. Phys. Lett*. **1998**, *290*, 519−525.
(13) Sosa, G. L.; Peruchena, N.; Contreras, R. H.; Castro, E. A. *THEOCHEM* **1997**, *401*, 77−85.
(14) Avendano, C.; Espada, M.; Ocana, B.; Garcia-Granda, S.; del Rosario Diaz, M.; Tejerina, B.; Gomez- Beltran, F.; Marinez, A.; Elguero, J. *J. Chem. Soc., Perkin Trans. 2* **1993**, 1547−1555.
(15) Marjo, C. E.; Bishop, R.; Craig, D. C.; Scudder, M. L. *Eur. J. Org. Chem*. **2001**, 863−873.
(16) Schmuck, S.; Lex, J. *Eur. J. Org. Chem*. **2001**, 1519−1523.
(17) Ochsenbein, P.; Bonin, M.; Schenk, K.; Froidevaux, J.; Wytko, J.; Graf, E.; Weiss, J. *Eur. J.Inorg. Chem*. **1999**, 1175−1179.
(18) Allerhand, A.; Schleyer, P. v. R. *J. Am. Chem. Soc*. **1963**, *85*, 1715−1723.
(19) Kariuki, B. M.; Harris, K. D. M.; Philip, D.; Robinson, J. M. A. *J. Am. Chem. Soc*. **1997**, *119*, 12679−12680.

10.1021/jo048592h CCC: $30.25 © 2005 American Chemical Society
Published on Web 11/26/2004

There are several experimental NMR evidences of intramolecular hydrogen bonds involving methylene, methine, and vinylic C−H groups.[7,14,21,22] Thus, the hydrogen bonds involving strongly activated methine protons in derivatives (**1**) were shown to promote stabilization of the six-membered rings in solution.[7] The α-proton of the vinyl group attached to a heteroatom (O, N, S) was shown to form a hydrogen bond with the neighboring donor atoms in various heterocyclic derivatives of which compound **2** is a representative example.[21,22] However, the experimental data on the aromatic C−H···X interactions are limited. Thus, it was found that 9-(2-pyrimidinyl)-9*H*-carbazole (**3**) features a dihedral angle of 7.4° between the aromatic planes, whereas the corresponding angle in 9-phenyl-9*H*-carbazole amounts 73.0°. This observation, together with the results of ^{1}H and ^{13}C NMR study and AM1 calculations strongly support the existence of C_{Ar}−H···N hydrogen bonds in derivative **3**.[14] Noteworthy, there are no accepting substituents in the carbazole moiety to activate the C−H bond involved in the interaction. The only example of the C_{Ar}−H···O hydrogen bond existence in benzobenzanthrone **4** corroborated mostly by a strong downfield shift of the proton involved in the interaction was given in.[28]

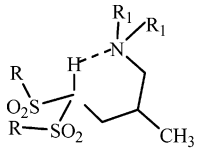

1

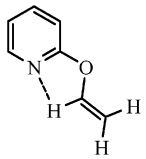

2

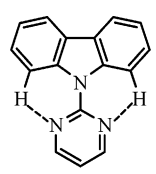

3

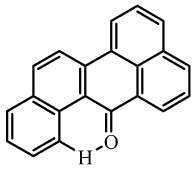

4

Ab initio and DFT calculations were used[27] to analyze the hydrogen bonds in model complexes between $F_nH_{3-n}C$−H and water, methanol, and formaldehyde as acceptors. Close similarities in behavior of C−H···O interactions with the conventional O−H···O hydrogen bond were found, in particular, similar equilibrium geometry and electron density changes. It was concluded that C−H···O interaction is a true hydrogen bond.

The hydrogen bond is usually described in terms of electrostatic attraction between the positive end of the bond dipole of the hydrogen donor moiety and the negative charge of the acceptor atom.[29] Therefore, it was claimed[29] that the presence of strong accepting substituents in the vicinity of the C−H group is a necessary condition for formation of the C−H···X bond.

Recently, we determined the structures of several products of 1,3-indandione self-condensation **5**−**13** (Chart 1).[30] The simplest molecule of the series, bindone (2-(3-oxo-2,3-dihydro-1*H*-inden-1-yliden)-1*H*-indene-1,3(2*H*)-dione, **5**), contains three strongly electron-accepting carbonyl groups, which according to ref 29 should increase the ability of the aromatic C−H bonds to form hydrogen bonds. All compounds of the series involve similar to bindone structural fragments. The detailed study of the series (**5**−**13**) and some model compounds (**14**−**17**) offers the unique opportunity to follow the influence of variations of hydrogen bond geometrical parameters on spectroscopic properties, in particular, the ^{1}H and ^{13}C NMR parameters.

Results and Discussion

Molecular Geometry and Hydrogen Bonds. There are a number of geometric criteria derived from the crystallographic data, which set limits for possible C−H···O hydrogen-bonding occurrence.[4] These are distances R and r as well as angles θ and φ:

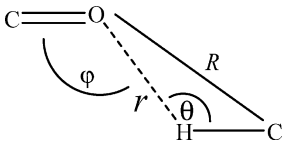

It is recognized[4] that the relevance of hydrogen bonding is justified if the fragment under consideration satisfied to the following range of parameters: R, 3.0 − 4.0 Å; r, 2.0−2.8 Å; θ, 110−180°; φ, 120−140°.

According to the earlier X-ray structure determination,[33] bindone molecule **(5)** is almost planar with the angle between the indan fragments about 4.5° and the length of the central double bond close to normal (1.34 Å). The C···O distance between C-7 and oxygen of the neighboring carbonyl group (R = 2.955 Å) is the shortest within the above-mentioned accepted range of the hydrogen-bonding relevance, and the angles θ and φ are 138.4 and 117.0, respectively. Recently, we found that bindone crystallizes in two polymorphic modifications, for which the X-ray structure determination was carried out at −80 °C.[34] The new polymorph involved two indepen-

(20) DeLaat, A. M.; Ault, B. S. *J. Am. Chem. Soc*. **1987**, *109*, 4232−4236.
(21) Afonin, A. V.; Sigalov, M. V.; Korostova, S. E.; Aliev, I. A.; Vashchenko, A. V.; Trofimov, B. A. *Magn. Reson. Chem*. **1990**, 580−586. Afonin, A. V.; Vashchenko, A. V.; Fujiwara, H. *Bull. Chem. Soc. Jpn*. **1996**, *69*, 933−945.
(22) Afonin, A. V.; Vashchenko, A. V.; Tatsuya, T.; Kimura, A.; Fujiwara, H. *Can. J. Chem.* **1999**, 416−424. Afonin, A. V.; Ushakov, I. A.; Kuznetsova, S. Yu.; Petrova, O. V.; Schmidt, E. Yu.; Mikhaleva, A. I. *Magn. Reson. Chem.* **2002**, *40*, 114−122.
(23) Lin, C.-H.; Yan, L.-F.; Wang, F.-C.; Sun, Y.-L.; Lin, C.-C. *J. Organomet. Chem*. **1999**, *587*, 151−159.
(24) Mele, A.; Vergani, B.; Viani, F.; Meille, S. V.; Farina, A.; Bravo, P. *Eur. J. Org. Chem*. **1999**, 187−196.
(25) Koch, U.; Popelier, P. L. A. *J. Phys. Chem*. **1995**, *99*, 9747−9754.
(26) Alkorta, I.; Campillo, N.; Rozas, I.; Elguero, J. *J. Org. Chem*. **1998**, *63*, 7759−7763.
(27) Gu, Y.; Kar, T.; Schneider, S. *THEOCHEM* **2000**, *500*, 441−452.
(28) Abliz, Z.; Moriyama, H.; Aoki, J.; Ueda, T. *Sci. China, B: Chem.* **1996**, *39*, 285−291.
(29) Hibbert, F.; Emsley J. *Adv. Phys. Org. Chem*. **1990**, *26*, 255−379.
(30) Jacob, K.; Sigalov, M.; Becker, J. Y.; Ellern, A.; Khodorkovsky, V. *Eur. J. Org. Chem*. **2000**, 2047−2055.
(31) Luef, W.; Keese, R. *Top. Stereochem*. **1991**, *20*, 231.
(32) Miehe, G.; Suesse, P.; Kupcik, V.; Egert, E.; Nieger, M.; Kunz, G.; Gerke, R.; Knieriem, B.; Niemeyer, M.; Luettke, W. *Angew. Chem., Int. Ed. Engl.* **1991**, *30*, 964−967.
(33) Bravic, G.; Bravic, G.; Gaultier, J.; Hauw, C. *Cryst. Struct. Commun*. **1976**, *5*, 5−8.
(34) Ellern, A.; Khodorkovsky, V. Unpublished results.

CHART 1. Compounds Studied in This Work

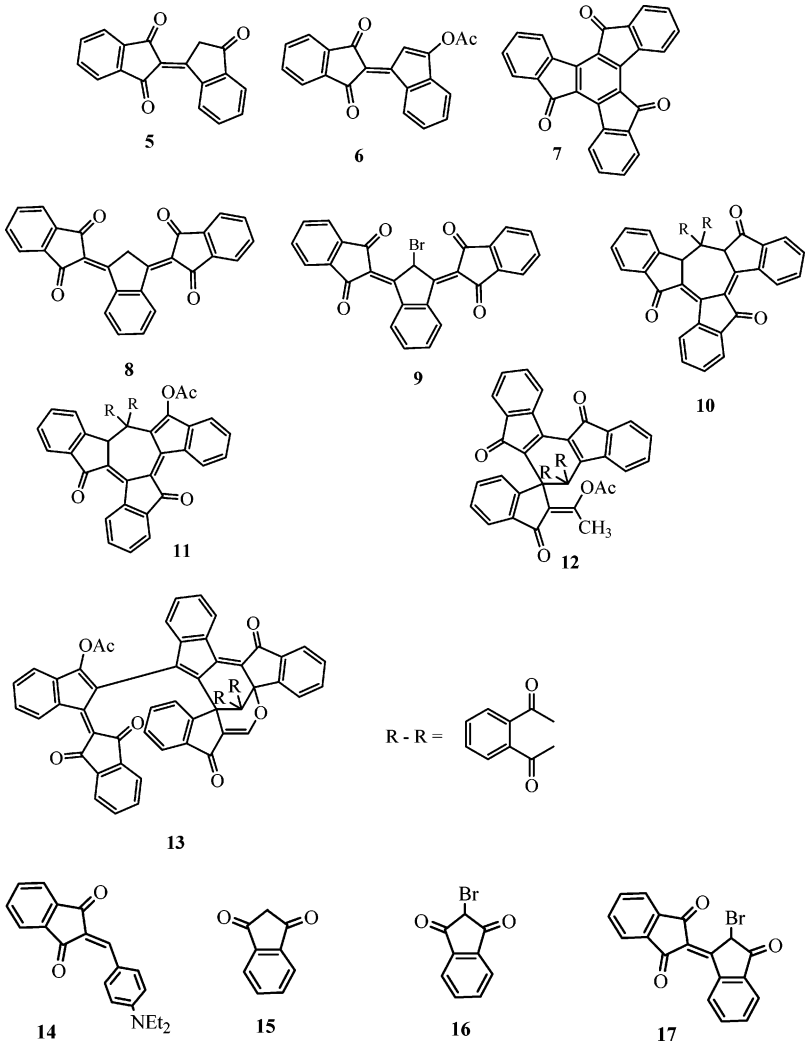

dent molecules per unit cell. The main geometric parameters related to hydrogen-bonded fragment in these two crystal forms of bindone are the length of connecting double bond (1.347 and 1.356 Å), C···O distance (2.940 and 2.958 Å), O···H distance (2.14 and 2.25 Å), and dihedral angle (2.2° and 6.5°). These results demonstrate that the central double bond is enough flexible to allow twisting of the two indene moieties and it can adopt a less planar conformation if the repulsion between H and O atom exists.

Indeed, several examples of strongly twisted C=C bonds are known,[31] and for instance, in *N*,*N*′-dimethylindigo **18**,[32] which is isostructural to bindone in the double bond vicinity, the length of the double bond connecting the two five-membered rings is 1.376 Å and the angle between them amounts to 26°.

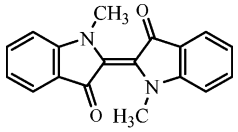

18

Moreover, in the derivative **13**, according to available X-ray data[30] the similar dihedral angle in acetylated bindone fragment amounts 11.4°.

At any rate, the bindone geometry cannot be considered as fully forced as in the case of benzobenzanthrone **4**.[28] For the set of derivatives involved in the present investigation, the experimental C···O distances are in the range of 2.86−3.05 Å, which fits to the above crystallographic definition of the hydrogen bond.

The Experimental and Calculated NMR Spectra of Bindone and Its Analogues. The full assignment of the ^{1}H NMR spectra and the detailed discussion related to structure identification of compounds **5**−**13** were reported previously.[30] A large downfield shift of one or two aromatic proton signals is the most remarkable feature of the ^{1}H NMR spectra of these compounds. The comparison of the ^{1}H chemical shifts in bindone and 1,3-indandione (Chart 2) shows that all ring protons except one remain almost unaffected when the carbonyl group is replaced by the 1,3-indandione moiety. Thus, in the spectrum of bindone (**5**), the proton spatially closest to carbonyl group gives a signal at 9.69 ppm, which is shifted by about 1.8 ppm downfield from the signal of its para-counterpart (7.90 ppm) experienced approximately the same electronic influence of substituents.

Another possibility to evaluate the influence of the neighboring carbonyl group on the ^{1}H NMR chemical shifts is offered by the low-temperature study of the model compound, 2-(4′-diethylaminobenzylidene)-1,3-in-

CHART 2. Chemical Shifts of Aromatic Protons in Bindone (5) and 1,3-Indandione (15)

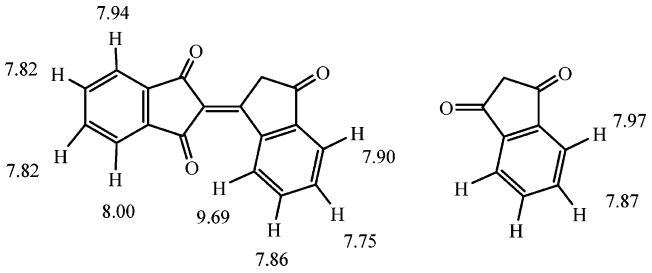

dandione **14**, which is isostructural to bindone at the vicinity of the carbonyl group. At 190 K, the aryl protons 2′ and 6′ become nonequivalent owing to slow rotation of the aryl group and the difference between their chemical shifts amounts 1.9 ppm.

Thus, two independently obtained values of 1.9 and of 1.8 ppm for close structural analogues can serve as the estimation of the neighboring carbonyl group effect.

Use of the crystallographic data for drawing the spectra−structure correlations for molecules in solution is recognized as limited, since the crystal lattice is known to strongly affect the molecular geometry. The geometry-optimized at a sufficiently high level of theory structures are free of the distortions induced by the crystal lattice, and one can expect the existence of a better correlation between the geometry and spectral parameters. We have optimized the bindone geometry using semiempirical (AM1, PM3), ab initio (HF/3-21G, HF/6-31G(d,p), HF/6-31G(2d,2p), HF/6-311G(2d,p)), MP2/6-31g(d,p), and DFT (B3LYP/6-31G(d,p), B3LYP/6-311G(2d,p), PBE1PBE/6-31G(d,p)) methods, see the Supporting Information Table S1.

Unexpectedly, all the methods failed to reproduce the experimental nonplanar geometry of this molecule. Noteworthy, all methods, including DFT, which gave the lowest standard deviation for the bond lengths, produced very short H···O distances (about 2.0−2.1 Å). Consequently, the calculated chemical shifts of all aromatic protons are in reasonable agreement with experimental values, except for the proton involved in the C−H···O interaction the ^{1}H NMR shift of which was predicted to amount 10.36 ppm, i.e., by 0.67 ppm larger than the experimental value (Table 1).

As expected, the attempt to use the X-ray geometry for the NMR calculations, gives rise to even larger disagreement between the calculated and experimental chemical shifts (Table 1). However, the chemical shift deviations are not uniform for all protons and especially carbons, but strongly depend on their position in the molecule. Thus, the deviation for "external" hydrogens and carbons 6, 7, 15, and 16 are much larger than for "internal" nuclei 5, 8, and 14, and also 4, 9, 13, and 18. This finding probably indicates that the "internal" parts of molecule are affected by the crystal force field in a lesser extent than the "external" ones. We also performed the partial optimization (HF/6-31G(d,p)) of a nonplanar bindone molecule with fixed distances O···H (2.20 Å) and O···C (2.955 Å) corresponding to experimental X-ray values.[33] All other bonds and angles were optimized. The chemical shifts, both ^{1}H and ^{13}C (except the carbonyl carbons), calculated for the partially optimized structure,

TABLE 1. Experimental and Calculated ^{1}H NMR Chemical Shifts for Bindone

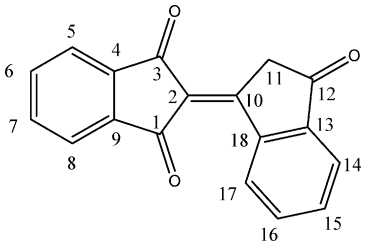

		B3LYP/6-31G(2d,2p) calcd for the following geometry:		
	expt ($CDCl_3$)	expt (X-ray)	HF/6-31G(d,p) fully optimized	HF/6-31G(d,p) partially optimized[a]
H-5	8.03	7.67	8.00	8.01
H-6	7.83	7.19	7.75	7.75
H-7	7.83	6.50	7.77	7.77
H-8	7.99	7.80	8.08	8.06
H-11	4.18	1.00	3.75	3.73
H-14	7.98	7.20	8.00	8.01
H-15	7.82	6.50	7.74	7.72
H-16	7.87	6.57	7.85	7.82
H-17	9.69	8.47	10.36	9.48
C-1	189.28	189.3	185.9	185.1
C-2	125.79	127.7	127.5	126.4
C-3	190.98	191.7	186.5	186.3
C-4	141.19	140.5	141.0	141.2
C-5	123.35	122.2	122.7	122.7
C-6	135.31	128.7	132.8	132.7
C-7	135.29	126.8	132.3	132.3
C-8	123.45	112.6	122.0	122.9
C-9	141.59	142.3	141.6	141.3
C-10	156.33	159.5	159.3	158.9
C-11	43.4	39.4	46.2	46.7
C-12	200.96	200.8	193.7	192.2
C-13	140.34	141.8	140.3	140.8
C-14	123.00	121.1	122.8	122.8
C-15	134.13	127.2	132.5	132.1
C-16	135.35	127.3	132.9	133.0
C-17	131.63	128.6	132.7	132.1
C-18	145.82	146.3	145.5	145.1

[a] Partially optimized with fixed O···H and C···O distances (see text).

are in excellent agreement with the experiment. One can assume that this structure is the best model of the real geometry in solution, where the equilibrium between the planar and twisted conformations may exist. The parameters R, r, θ, and φ are in agreement with the geometric criteria[4] of hydrogen bonding. The energy differences between the fully optimized and partially optimized bindone molecules are 0.8 kcal/mol for the HF/6-31G(d,p) method and 1.1 kcal/mol for B3LYP/6-31G(d,p).

The low-field shifted signals of the C−H groups of other analogues cover the range from 9.83 ppm for compound **8** to 8.75 ppm for **13** (Table 2). Taking into account the electron-accepting character of substituents in all these compounds, one can assume that the main reason for the observed wide range of chemical shifts is the differences in the geometry within the series, i.e., in distances R, r, angles θ, φ, and the dihedral angles between the indene moieties.

The data for compounds **5**,[33,34] **9**, **11**, and **13**[30] (Table 2) show that the geometries of the CH···O=C fragments indeed differ significantly; in particular, the distance O···C varies from 2.86 to 3.05 Å. There is a rough trend in

TABLE 2. ^{1}H NMR Chemical Shifts of the Low-Field Proton, ^{13}C of the Corresponding Carbon, the Experimental (X-ray) R (O···C) Distances and Optimized (HF/6-31g(d,p)) Geometric Parameters at the C=O···H−C Vicinity

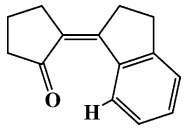

compd	δ ^{1}H, ppm expt and (calcd)[a]	δ ^{13}C−H···O, ppm [^1J(^{13}C−^{1}H)] Hz	R (O···C) expt, Å (calcd)	r (O···H), calcd, Å	θ calcd, deg	φ calcd, deg
5	9.69	131.67 [170.0]	2.95[33]	2.06	138.4	117.0
	(10.36)		(2.95)			
6	9.16[b]		(2.95)	2.09	135.6	119.1
	(9.73)					
7	9.31	131.88	(3.03)	2.16	136.8	117.2
	(9.73)					
8	9.83	131.30	(2.94)	2.03	141.6	115.1
	(10.66)					
9	9.61	131.80 [170.0]	2.92[30]	2.13	131.2	113.8
			(2.94)			
10[c]	9.60	130.70 [171.0]	(2.96)	2.14	131.3	115.2
	(9.99)					
	9.46	128.46 [170.0]	(2.96)	2.15	130.8	118.0
	(9.83)					
11	9.62		2.86[30]	2.11	128.7	118.3
			(2.90)			
	9.00[b]		2.92[30]	2.06	133.0	116.1
			(2.89)			
12	9.13		(3.02)	2.14	135.1	115.7
13[d]	8.75[b]		3.05[30]	2.13	135.8	116.3
			(3.02)			
	9.26[b]		2.87[30]	2.10	118.1	110.3
			(2.80)			

[a] B3LYP/6-31G(2d,2p)//HF/6-31G(d,p). [b] Omitted in correlation. [c] The corresponding protons are marked as 10-1 and 10-2 in Figure 1. [d] AM1 optimization.

affecting the ^{1}H NMR chemical shifts by the O···C distance; for example, the low-field signals in the spectra of derivatives **5**, **9**, and **11** (one of two signals) have rather close chemical shift values of 9.69, 9.61, and 9.62 ppm. The corresponding O···C distances are also very close—2.87−2.88 Å. The largest experimental distance of 3.05 Å in one of two C−H···O=C fragments of derivative **13** is in accordance to the smallest downfield signal displacement of 8.75 ppm.

Unlike in the case of bindone, we cannot carry out the similar analysis of partially optimized structures because of the lack of the precise X-ray data for the other compounds of the series. We carried out the geometry optimization and the ^{1}H NMR chemical shifts calculations for several representative compounds of the series in order to evaluate how this overestimation depends on molecular geometry. The corresponding HF/6-31G(d,p)-optimized geometrical parameters and calculated chemical shifts of C−H···O proton are also given in Table 2. Although the optimized structures are free of distortions induced by the crystal lattice, the calculations apparently systematically overestimate the chemical shifts of the protons involved in the hydrogen bonds, as was the case with bindone.

Let us compare the changes of relative orientation of hydrogen-bonded fragments and consider the "dihedral" angle C−H···O=C as the measure of this orientation. For optimized structures, the values of this angle are 0° for compounds **5**−**8**, 49° for **9**, 21° and 31° for two fragments of **10**, and 36° and 4° for two fragments of **11**. This variety of geometries gives rise to the variations in the nonbonding factors affecting the ^{1}H chemical shifts, such as carbonyl group anisotropy, electric field and steric effect (see below), which within the series of compounds **5**−**11** cannot be taken into account explicitly.

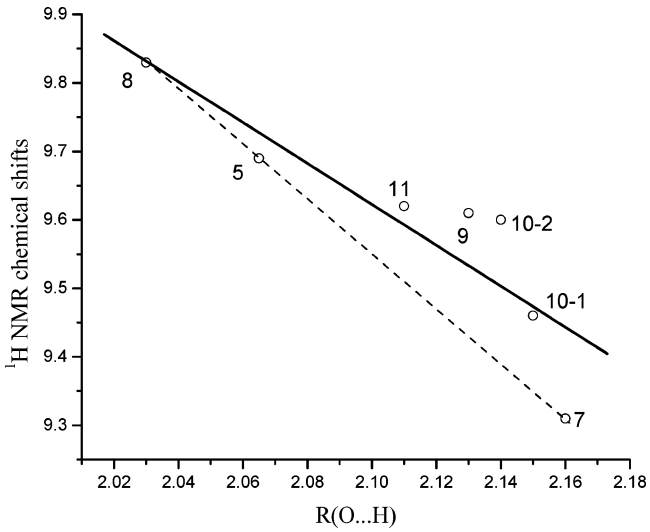

FIGURE 1. Experimental chemical shifts dependence on calculated O···H distances. The point numbers correspond to Chart 1 and Table 2. —: linear fit for all data (r = −0.886). − −: linear fit for the fully planar molecules.

These considerations explain why only a rough correlation between the experimental chemical shift of the low-field proton signal and the optimized (HF/6-31G(d,p)) O···H distance for derivatives **5** and **7**−**11** (Figure 1) is observed. The experimental points corresponding to the acetylated bindone fragments (compounds **6** and **11**) were

CHART 3. Experimental and Calculated (in Parentheses) ^{1}H NMR Chemical Shifts for 6−8

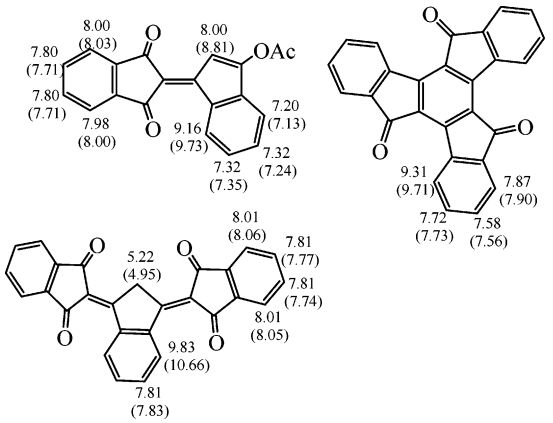

omitted as the slightly donating acetoxy group brings about the high-field shifts of all aromatic protons as it was mentioned previously.[30] However, the data for the nonacetylated fragment of compound **11** were included into the correlation. AM1 optimization for the large molecule **13** was performed, and the data are also omitted from the correlation.

Moreover, the linear dependence is observed for the compounds **5**, **7**, and **8** (Figure 1, dashed line) and it is the direct consequence of the fact that for these fully planar molecules the only factor affecting ^{1}H NMR chemical shifts is O···H distance.

The calculated ^{1}H NMR chemical shifts for all aromatic hydrogens, which are not located in the proximity of the oxygen atom, are in excellent agreement with the experimental data (Chart 3).

Hydrogen Bond Contribution in the ^{1}H NMR Chemical Shifts. The overall effect of the neighboring carbonyl group on the ^{1}H NMR chemical shifts involves, besides the contribution of the hydrogen bond, also nonbonded interactions such as carbonyl magnetic anisotropy and steric and electric field influence. For evaluating the proton chemical shifts, a general semiempirical scheme including these effects was developed[35] and applied to aromatic carbonyl derivatives.[36]

The carbonyl magnetic anisotropy term was obtained from the solution of the Mc-Connell equation (1)

$$\delta_{\text{anis}} = [\Delta\chi_{\text{par}}(3\cos^2\theta_1 - 1) + \Delta\chi_{\text{perp}}(3\cos^2\theta_2 - 1)]/3R^3 \quad (1)$$

where R is the distance between the center of the C=O bond and the proton and θ_1 and θ_2 are angles between the radius vector R and the molecular axes X_1 and X_3 (Figure 2).

The value of oxygen steric influence was calculated by equation (2)

$$\delta_{\text{steric}} = a_s/r^6 \quad (2)$$

where r is the distance between proton and oxygen.

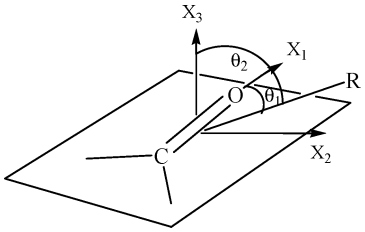

FIGURE 2. Model for calculation of the carbonyl group anisotropy.

The calculation of the electric field effect was accomplished using equation (3)

$$\delta_{\text{el}} = A_z E_z \quad (3)$$

where E_z is the component of the electric field along the C−H bond.

Taking into account the close similarity of the compounds studied in this work, and the compounds described in[36] the factors $\Delta\chi_{\text{par}}$, $\Delta\chi_{\text{perp}}$, a_s, and A_z were adopted from[36] 6.36×10^{-30}cm^3 molecule^{-1}, -11.88×10^{-30}cm^3 molecule^{-1}, 38.4 ppm Å,[6] and 3.67×10^{-12} esu, respectively.

Using these values and the above-mentioned partially optimized geometry of bindone (**5**), for which the carbonyl group influence amounts 1.8 ppm, we calculated the contributions of the magnetic anisotropy and steric and electric field effects, which amount to 0.31, 0.33, and 0.55 ppm, respectively. The difference between the measured value of 1.8 ppm and the sum of these effects (1.19 ppm) is about 0.6 ppm, which can be considered as the refined and reasonable measure of hydrogen bonding influence. The same calculations for other compounds were not performed because of the lack of suitable geometrical model for such calculations.

^{13}C Chemical Shifts and One-Bond Spin−Spin Coupling Constants $^1J(^{13}C-^1H)$. It is well-established[38] that ^{13}C chemical shifts and $^1J(^{13}C-^1H)$ of $CHCl_3$ in various solvents strongly depend on the donor properties of the solvent that was explained by the ability of chloroform to form hydrogen bonds. The variation of solvent from cyclohexane to pyridine leads to the 2.6 ppm carbon deshielding and about 7 Hz increase of $^1J(^{13}C-^1H)$.

The short discussion of data regarding increase of the spin−spin coupling constants $^1J(^{13}C-^1H)$ in the contacts of type C−H···M where M is an electronegative atom is given in the recent review.[39] It was concluded that there are contributions of both charge transfer and electrostatic effect.

(35) Abraham, R. J. *Prog. Nucl. Magn. Reson.* **1999**, *35*, 85−152.
(36) Abraham, R. J.; Mobli, M.; Smith, R. J. *Magn. Reson. Chem.* **2003**, *41*, 26−36.
(37) Frisch, M. J.; Trucks, G. W.; Schlegel, H. B.; Scuseria, G. E.; Robb, M. A.; Cheeseman, J. R.; Zakrzewski, V. G.; Montgomery, J. A., Jr.; Stratmann, R. E.; Burant, J. C.; Dapprich, S.; Millam, J. M.; Daniels, A. D.; Kudin, K. N.; Strain, M. C.; Farkas, O.; Tomasi, J.; Barone, V.; Cossi, M.; Cammi, R.; Mennucci, B.; Pomelli, C.; Adamo, C.; Clifford, S.; Ochterski, J.; Petersson, G. A.; Ayala, P. Y.; Cui, Q.; Morokuma, K.; Malick, D. K.; Rabuck, A. D.; Raghavachari, K.; Foresman, J. B.; Cioslowski, J.; Ortiz, J. V.; Stefanov, B. B.; Liu, G.; Liashenko, A.; Piskorz, P.; Komaromi, I.; Gomperts, R.; Martin, R. L.; Fox, D. J.; Keith, T.; Al-Laham, M. A.; Peng, C. Y.; Nanayakkara, A.; Gonzalez, C.; Challacombe, M.; Gill, P. M. W.; Johnson, B. G.; Chen, W.; Wong, M. W.; Andres, J. L.; Head-Gordon, M.; Replogle, E. S.; Pople, J. A. *Gaussian 98*, revision A.9; Gaussian, Inc.: Pittsburgh, PA, 1998.
(38) Lichter, R. L.; Roberts, J. D. *J. Phys. Chem.* **1970**, 912−916. Evans, D. F. *J. Chem. Soc.* **1963**, 5575−5577.
(39) Contreras, R. H.; Peralta, J. E. *Prog. Nucl. Magn. Reson.* **2000**, *37* (4), 321−425.

CHART 4. ^1H Chemical Shifts and One-Bond Coupling Constants $^1J(^{13}C-^1H)$ of Methylene and Methine Protons

Entry	R	$\delta(^1H)$	$J(^{13}C - ^1H)$
15	H	3.25	133.7
16	Br	4.86	154.5
5	H	4.18	135.6
17	Br	6.40	166.9
8	H	5.23	137.3
9	Br	8.42	173.8

The C−H···N hydrogen bond formation with participation of the α-vinyl proton in vinyl ethers[21,22] is accompanied not only by a downfield shift of participating proton (about 1 ppm) but also by increase (∼6−7 Hz) in the spin−spin coupling constant $^1J(^{13}C-^1H)$. The values measured for several representative compounds (**5**, **9**, **10**) of $^1J(^{13}C-^1H)$ were 170−171 Hz, whereas hydrogen atoms that are not involved in the interaction with carbonyl showed $^1J(^{13}C-^1H)$ ca. 162 Hz. The 8−9 Hz increase in the one-bond coupling $^{13}C-^1H$ is a considerable increment and can be definitely considered as the spectral evidence of hydrogen bonding.

The ^{13}C chemical shifts of these carbons (Table 2) are shifted by 8−9 ppm downfield compared to the other aromatic carbons at similar positions (122−123 ppm). A similar 5-ppm deshielding was detected but not discussed for carbazole carbons C_1 and C_8, which are involved in the C−H···N hydrogen-bonded moiety in 9-(2-pyrimidinyl)carbazole (**3**) as compared with 9-phenylcarbazole.[13] The same trend was revealed from comparison of the experimental and calculated ^{13}C chemical shifts in bindone − the calculated deshielding effect on the carbon in the hydrogen-bonded moiety (about 9 ppm) reproduces well the experimental one (Table 1).

However, neither ^{13}C NMR chemical shifts nor one-bond $^{13}C-^1H$ coupling constants in Table 2 show any reasonable dependence on the proton chemical shifts and on the calculated O···H distance.

Hydrogen Bonds C−H···O with the Participation of Nonaromatic Protons. As mentioned above, many examples of such interaction involve activated methylene or methine protons in the presence of substituents increasing their hydrogen bonding ability. The methine proton in bis-phenylsulfonyl methane (**1**) derivatives was shown to form strong intramolecular hydrogen bonds with the remote nitrogen atom.[7] The methylene protons within compounds **5** and **7**, despite their activated nature, do not exhibit any features of the hydrogen bonding.

The consecutive replacement of the carbonyl O atoms in the indandione molecule with the 1,3-indandione-2-ylidene moiety results in rather small increase in the one-bond coupling $^1J(^{13}C-^1H)$ and brings about almost additive shifts of these protons to the low field (Chart 4), the latter may be attributed to a stronger anisotropic influence of two nearer located carbonyl groups of the 1,3-indandione-2-ylidene moiety. Relatively long distances between hydrogens and oxygen (2.44−2.51 Å) and the small angles C−H···O (∼90°) predetermined by the near to planar backbone of these derivatives prevent any substantial C−H···O interaction.

In the series of bromo-substituted 1,3-indandione (**16**), bindone (**17**), and bis-(1,3-indandion-2-yl)indan (**9**), both the chemical shifts and spin−spin couplings of the methine protons are more sensitive to the change in their environment (Chart 4). The chemical shift difference between 1,3-indandione **15** and derivative **8** is 1.98 ppm, whereas in their bromo analogues **16** and **9** it amounts to 3.56 ppm. The change in the difference between the spin−spin coupling constants is very large (from 3.6 Hz for the pair of **15** and **5** to 19.3 Hz for the pair of **16** and **9**).

All of the above features can be explained by taking into account the corresponding structural changes. The geometry optimization (HF/6-31G(d,p) level) yielded a planar structure for **16**, and the planarity diminishes considerably for **17** and especially for **9** (the latter calculation is supported by the X-ray measurements). The repulsive electrostatic and dipole−dipole interaction of the bromine and two oxygen atoms result in a butterfly conformation. The methine proton in **9** is located almost in the plane formed by the two carbonyl groups and the distance between this proton and the both oxygen atoms is 2.24 Å, which is sufficient for effective C−H···O bond formation. The orbital structure analysis corroborates this assumption.

Orbital Structure. As mentioned above, the usual description model of hydrogen bond is electrostatic attraction between donor and acceptor.[29] The requirement of strong accepting substituents nearby to C−H bond participating in hydrogen-bond formation is the direct consequence of this model. Strong activating influence of substituents is observed, for example, in the chloroform which is well-known as hydrogen-bond donor[38] and in derivatives **1** considered in the Introduction. On the other hand, in the carbazole derivative **3** where the hydrogen bonding is established,[14] the nitrogen atom closest to C−H bond is donor rather than acceptor substituent. The carbonyl groups in compounds **5**−**13** do not affect as strongly as sulfonic groups in **1**, and thereby the demand claimed in ref 29 is not implemented.

These considerations prompt us to examine the possibility of partially covalent nature of hydrogen bonds. From a quantum mechanical point of view it means the non-zero probability of finding electrons in the space between the carbonyl oxygen and hydrogen atoms of the C−H group.

The coefficients of the orbital overlap are given in Chart 5. In every case, the signs of the coefficients are positive, meaning the attractive character of the interaction.[40] The overlap coefficient between the O and H atoms within molecule **5** amounts 0.063. The corresponding coefficients for the methylene atoms CH_2, which are not involved in hydrogen bonding with the nearest oxygen atom owing to the large H···O distance and the small

(40) Clark, T. *A Handbook of Computational Chemistry*; John Wiley & Sons: New York, 1990.

CHART 5. Orbital Overlap of Atoms in CH···O Fragments

Compound	Pair of atoms*	Overlap coefficient	Interatomic distance
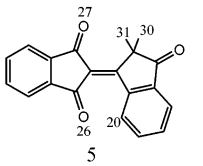 5	O(26)… H(20)	0.0631	2.06
	O(27)… H(30,31)	0.0065	2.54
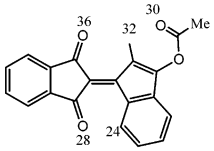 6	O(28)… H(24)	0.0631	2.09
	O(36)… H(32)	0.0480	2.23
	O(30)… H(32)	0.0270	2.39
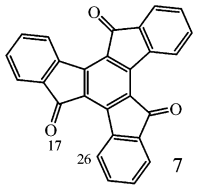 7	O(17)… H(26)	0.0609	2.16
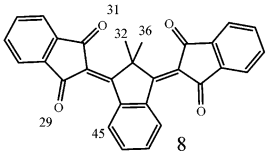 8	O(29)… H(45)	0.0658	2.03
	O(31)… H(32,36)	0.0071	2.51
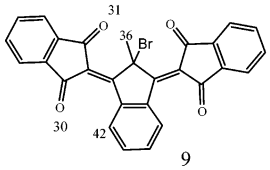 9	O(30)… H(42)	0.0518	2.13
	O(31)… H(36)	0.0411	2.24

[a] Atom numbering used in calculations is given (see the Supporting Information).

angle θ, are 10 times smaller (0.0065). The similar coefficients were calculated for the linear indandione trimer **8**. Indeed, the corresponding coefficient for the methine hydrogen of the brominated analogue **9**, with the shorter H···O distance, is considerably larger, in agreement with the discussed above change in the geometry.

The overlap coefficient for acetylbindone **6** has a usual for this series value of 0.063. It should be noted for this compound that according to the overlap coefficient the ability of its aromatic hydrogen to form hydrogen bond is the same as for bindone and the chemical shift deviation (see above) is not related to hydrogen bonding.

The olefinic hydrogen in **6**, which can be involved in the bifurcated hydrogen bonding, has the overlap coefficients of 0.048 and 0.027, respectively.

The satisfactory linear dependence between the overlap coefficients and the calculated O···H distances is observed (Figure 3)

It should be emphasized that there is no correlation between the orbital overlap coefficients and chemical shifts of the low-field proton, which also evidences the complex nature of the NMR shielding in hydrogen-bonded systems.

Figure 4 shows an example of such overlap in the bindone HOMO^{-49} orbital.

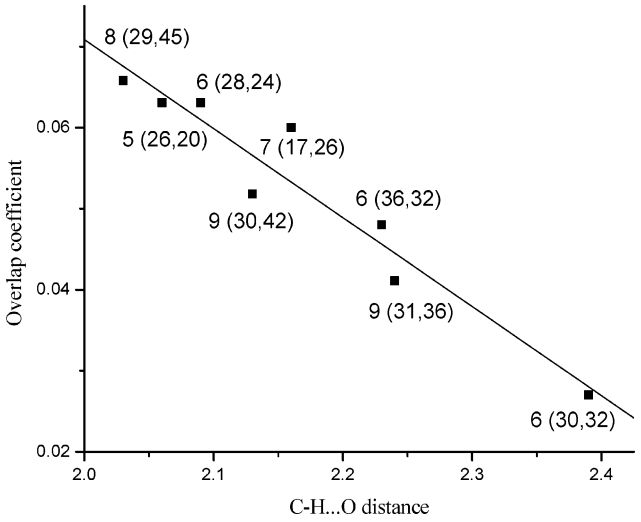

FIGURE 3. Dependence between the orbital overlap and the calculated O···H distances ($r = -0.96$). The numbers of interacting atoms (in parentheses) correspond to Chart 5.

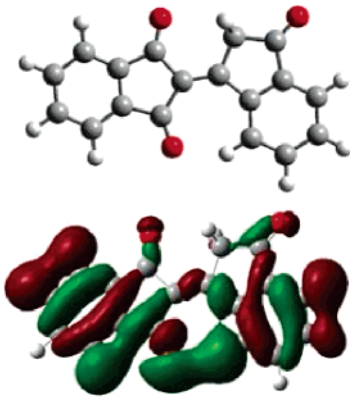

FIGURE 4. Bindone molecule (top) and the electron density surface of the HOMO^{-49} orbital (bottom).

Conclusion

The presence of the hydrogen-bonding C_{Ar}−H···O within the series of derivatives **5**−**13** is manifested by the strong downfield shifts of the corresponding protons by ca. 1.8 ppm. This effect is also corroborated by the quantum mechanical calculations. There is a rough correlation between the ^{1}H NMR chemical shifts and O···H distance and the highest observed shift of 9.83 ppm corresponds to the shortest distance of 2.03 Å, whereas the smallest shift of 9.31 ppm corresponds to the longest 2.16 Å distance. For bindone (**5**), the contribution of the hydrogen bond to the overall 1.8 ppm shift is estimated to amount 0.6 ppm. Unexpectedly, no definite trends in the ^{13}C chemical shifts and one-bond spin−spin coupling constants were found. Further studies on a more refined set of derivatives are underway in order to appreciate the energy of the C_{Ar}−H···O hydrogen bond.

Experimental Section

The ^{1}H and ^{13}C NMR spectra were recorded at 500 and 125 MHz, respectively, in $CDCl_3$ solutions. Assignment of ^{13}C signals of C−H···O fragments was performed by 2D HXCORR technique.

The quantum-mechanical calculations were performed with Gaussian 98W software.[37] ^{1}H and ^{13}C NMR chemical shifts were calculated by the GIAO method in the B3LYP/6-31G-(2d,2p) basis set for the HF/6-31(d,p)-optimized geometry.

The synthesis and NMR spectra of derivatives **5**−**13** were described earlier. [30] The model compound **14** was synthesized according to ref 41. 2-Bromobindone **17** was synthesized according to the published procedure.[42]

Supporting Information Available: NMR data for compounds **14** and **17**, optimized molecular geometries of bindone, and Cartesian coordinates and computed total energies for optimized structures **5**−**11**. This material is available free of charge via the Internet at http://pubs.acs.org.

JO048592H

(41) Khodorkovsky, V.; Mazor, R. A.; Ellern, A. *Acta Crystallogr.* **1996**, *C52*, 2878−2880.
(42) Hantzsch, A.; Zortmann J. *Lieb. Ann. Chem.* **1912**, *392*, 322.